

Lifetime and Landé factor measurements of $5p7p$ levels of Sn I by time-resolved laser spectroscopyYing Zhang,¹ Jiaxin Xu,¹ Wei Zhang,¹ Shuai You,¹ Zhiguo Ma,¹ Lili Han,¹ Pengfei Li,¹ Guijuan Sun,¹ Zhankui Jiang,¹ S. Enzonga Yoca,² P. Quinet,^{2,3} É. Biémont,^{2,3} and Zhenwen Dai^{1,*}¹Department of Physics, Jilin University and Key Laboratory of Coherent Light, Atomic and Molecular Spectroscopy, Ministry of Education, Changchun 130023, China²IPNAS (Bât. B15), Université de Liège, Sart Tilman, B-4000 Liège, Belgium³Astrophysique et Spectroscopie, Université de Mons-Hainaut, B-7000 Mons, Belgium

(Received 15 April 2008; published 7 August 2008)

Lifetimes for nine levels and Landé g_J factors for eight levels of the $5p7p$ configuration of neutral tin have been measured by the time-resolved fluorescence method and by the Zeeman quantum beat technique, respectively. A two-step laser excitation technique has been used for the measurements. The results obtained are compared with relativistic Hartree-Fock lifetime and g_J values taking core-polarization effects into account.

DOI: 10.1103/PhysRevA.78.022505

PACS number(s): 32.70.Cs, 42.62.Fi, 32.10.Dk, 31.15.-p

I. INTRODUCTION

Neutral tin (Sn I, $Z=50$), which belongs to the carbon group elements, is characterized by a $5s^25p^2$ ground configuration. The first excited configurations of the same atom consist of an nl electron outside of a $5p$ electron ionic core (Sn II), the ground configuration $5s^25p$ of the ion core giving rise to two ionization limits: $^2P_{1/2}^o$ ($59\,232.69\text{ cm}^{-1}$) and $^2P_{3/2}^o$ ($63\,484.18\text{ cm}^{-1}$) [1]. Despite of its rather simple structure, the electronic spectrum of Sn I has been investigated by rather few authors. Moore [2] summarized early data, while Brill [3] and Wilson [4] studied the atomic structure of Sn I using the arc and absorption techniques, respectively, but unfortunately their results were not presented. In 1977, Brown *et al.* [1] determined numerous odd-parity levels from a high-resolution absorption spectrum observed between 158 and 204 nm. Recently, utilizing two-step laser spectroscopy, Nadeem *et al.* [5,6] investigated the $5pnp$ ($1/2, 3/2$)₂ ($11 \leq n \leq 56$), $5pnp$ ($1/2, 3/2$)₁ ($12 \leq n \leq 18$), $5pnp$ ($1/2, 1/2$)₁ ($20 \leq n \leq 31$), and $5pnf$ ($1/2, 5/2$)₂ ($12 \leq n \leq 46$) even-parity Rydberg levels as well as some $5p8p$ and $5p5f$ levels. In addition, many $5pnp$ and $5pnf$ autoionizing levels of Sn I have been reported by the same group [7]. Jin *et al.* [8] measured $5pnp$ and $5pnf$ even-parity Rydberg levels with $J=0$ to 3 using the resonant multiphoton ionization time-of-flight mass spectroscopy (TOFMS) method, but no detailed results were reported by these authors. The $5s5p^3$ configuration of Sn I, which strongly interacts with the $5s^25pns$ and $5s^25pnd$ configurations, has been discussed in detail by Dembczynski and Rebel [9] and by Dembczynski and Wilson [10].

In astrophysics, Sn isotopes are produced by the p , s , and r processes. Tin has been identified in the photospheric solar spectrum and in the spectra of some chemically peculiar hot stars (i.e., in Ap stars) [11]. More recently, the absorption feature at 380.102 nm was investigated in the near ultraviolet (uv) spectrum of HD 221170 [12] as part of a strategy to get a deeper understanding of the nature of r -process-rich stars. A quantitative investigation of stellar spectra requires how-

ever accurate radiative data for the transitions of astrophysical interest.

In order to get more insight into the properties of excited states of Sn I, additional atomic structure data, such as natural radiative lifetimes, Landé g_J factors as well as hyperfine structure information, are required. Although some efforts have been devoted to the investigation of selected Sn I levels, data concerning lifetimes and Landé factors of this atom are still extremely scarce. The main reason for this situation results from the fact that a high-temperature source is needed to obtain an atomic beam with sufficient vapor density usable in a spectroscopic experiment. Furthermore, for even-parity levels, the states worth of consideration for intermediate resonance are accessible through wavelengths located in the uv region and their lifetimes are very short (only a few nanoseconds). For odd-parity levels, most resonant lines lie in the uv and vacuum ultraviolet (vuv) regions and hence it is rather difficult to excite the corresponding levels.

As far as we know, in the literature, radiative lifetimes of only nine low-lying odd-parity levels in $5p6s$ and $5p5d$ have been measured using different techniques including the Hanle-effect method, beam-foil spectroscopy, the phase-shift approach, and Rozhdestvenskii's hook method [13–17]. Among the levels investigated, the lifetime of the $5d\ ^3F_2$ level is reaching 24 ns while all the other values are not longer than 7 ns.

Landé g_J factors of $5p^2$, $5p6s$, $5p5d$, $5p7s$, and $5p6d$ levels have been compiled by Moore [2], these results being based on early results presented by Back [18], Green and Loring [19], and Meggers [20] and deduced from observations of the Zeeman effect. It should be emphasized however that, except for the ground configuration, the presented Landé factors concern only very few odd-parity levels.

From the above discussion, it is obvious that characteristic physical quantities of even-parity levels in Sn I are strongly needed. These data are very important not only for atomic spectroscopy but also for astrophysical applications. As a consequence, in this paper, we report on an experiment to determine the lifetimes and Landé g_J factors of high-lying even-parity levels in the $5p7p$ configuration of Sn I using a time-resolved laser-induced fluorescence technique and Zeeman quantum-beat spectroscopy in an atomic beam. The

*Corresponding author; dai@jlu.edu.cn; FAX: 86 431 88941554.

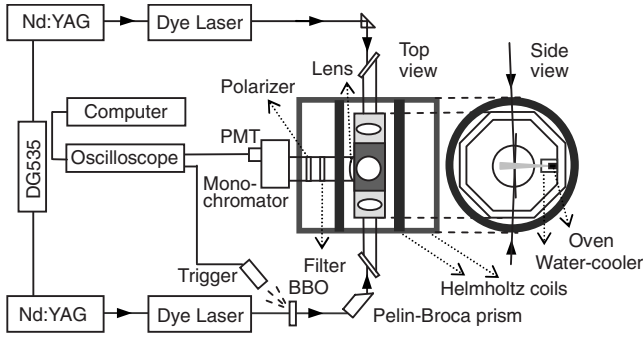


FIG. 1. Experimental setup for lifetime and Landé factor measurements.

natural radiative lifetimes of nine levels and the g_J factors of eight levels were obtained. The experimental lifetimes and Landé factors agree reasonably well with relativistic Hartree-Fock calculations provided core-polarization effects are adequately included in the theoretical model.

II. EXPERIMENTAL SETUP

The experimental setup used for the lifetime and Landé factor measurements is shown in Fig. 1. The diagram of energy levels and the detailed excitation schemes relevant to the present experiment are illustrated in Fig. 2. The energy levels were taken from tables given by Moore [2]. The exciting laser system consisted of two dye lasers (Sirah Cobra-Stretch) pumped, respectively, by two Q-switched Nd:YAG lasers working at a 10 Hz repetition rate and with about 8 ns pulse duration. One was a Nd:YAG 532 nm laser (Spectra-Physics Quanta-Ray Pro-Series) pumped by rhodamine 6G or DCM dyes, and the second was a Nd:YAG 355 nm laser

(Continuum Precision II) pumped by rhodamine 6G, coumarin 540A or coumarin 500 dyes. The linewidths of these two dye lasers were about 0.08 cm^{-1} .

A two-step excitation process was used to populate the even-parity $5p7p$ states as shown in Fig. 2. The $5p6s \ ^3P_1^o(34\ 914.282 \text{ cm}^{-1})$ and $\ ^3P_2^o(38\ 628.876 \text{ cm}^{-1})$ levels were used, respectively, as the intermediate states according to the levels under investigation. For the first step, a second-harmonic wave of a dye laser generated by a BBO type-I crystal was used. The rhodamine 6G dye laser was tuned at 572.8 nm to excite the $5p6s \ ^3P_1^o$ state from the $5p^2 \ ^3P_0$ ground state while the coumarin 540A dye laser was tuned to 541.5 nm to excite $5p6s \ ^3P_2^o$ from the $5p^2 \ ^3P_1$ metastable level (1691.806 cm^{-1}). For the second step, dye lasers operating with different dyes (rhodamine 6G, DCM, and coumarin 500) were used to excite the $5p7p$ levels in the energy range extending from $50\ 755.8$ to $55\ 500.6 \text{ cm}^{-1}$. The two laser beams were sent horizontally from opposite directions to cross at the center of the vacuum chamber, where they intersected the vertical atomic beam. Following the stepwise excitation, fluorescence light was collected by a convex lens in a direction perpendicular to the atom and laser beams and detected by a photomultiplier tube (PMT) (Hamamatsu R3896) after filtering by a grating monochromator. The time-resolved fluorescence photocurrent signal from the PMT was registered by a 500 MHz digital oscilloscope (Tektronix TDS 620B) and then transferred to a personal computer from which the lifetime can be obtained. In view of the short lifetimes of intermediate levels, which reach 4.75 and 4.25 ns for $5p6s \ ^3P_1^o$ and $\ ^3P_2^o$, respectively [13], it is necessary to make a proper time overlap of the two laser beams. The pulse durations of the two dye lasers were about 7 ns. A delay of 3–5 ns between the first and the second lasers was found not to affect significantly the fluorescence intensity. Therefore, this delay was adopted in the experiment with the effect of decreasing the laser-field-induced ac Stark effect by about 10% to 30%. Using a relativistic Hartree-Fock approach described in Sec. IV, the Stark shifts were roughly estimated for the levels considered in the present work under a laser electric field reaching about $5 \times 10^4 \text{ V/cm}$ and they were found to be -0.01 cm^{-1} for the level $34\ 914 \text{ cm}^{-1}$ and -0.7 cm^{-1} for the $5p7p$ levels. The delay control was achieved with the help of a digital delay generator (Stanford Research System Model 535).

A high-temperature resistively heated oven which can operate up to 1700 K was constructed for producing the atomic beam. A tin sample with purity of 99.8% was put in a corundum crucible located in a columniform sleeve wound using a molybdenum heating wire. On the crucible a corundum cover with a hole of 1.5 mm diameter at the center was placed for generating an atomic beam with a diameter of about 5 cm in the interaction region. The interaction region between the lasers and the atomic beam was about 15 cm above the spout.

A pair of Helmholtz coils was used to generate a homogeneous magnetic field, which can be up to 300 G, along the direction of fluorescence detection and at the same time parallel to the horizontal component of the earth’s magnetic field. Under this field, Zeeman splitting does affect the investigated levels. Besides, another pair of coils was employed to

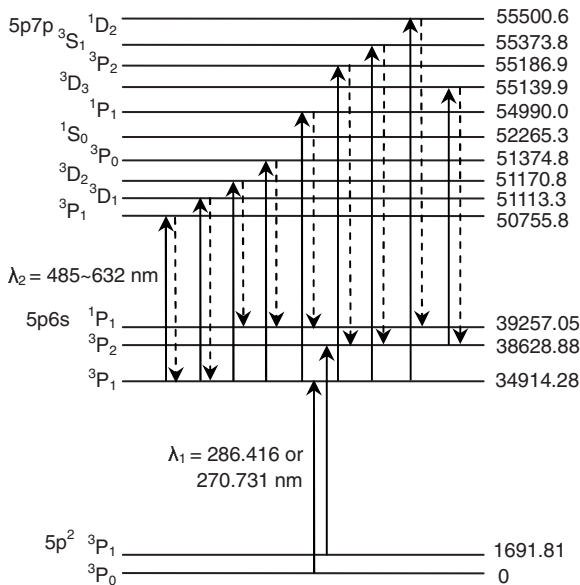


FIG. 2. Partial energy-level diagram of the Sn atom and excitation schemes. The solid lines indicate the excitation pathways, and the dashed lines show the fluorescence channels. Unit of energy levels is cm^{-1} .

TABLE I. Experimental lifetimes and Landé factors of Sn I $5p7p$ levels and comparison with the theoretical results.

E (cm ⁻¹) ^a	Term ^a	n^*	Lifetime (ns)			Landé factor		
			Expt.	HFR ^a		Expt.	HFR ^a	
				A	B		A	B
50755.8	$5p_{1/2}7p^3P_1$	3.598	262(8)	367	394	0.6652(27)	0.670	0.661
51113.3	$5p_{1/2}7p^3D_1$	3.676	163(8)	154	167	1.4631 (44)	1.468	1.477
51170.8	$5p_{1/2}7p^3D_2$	3.689	157(5)	137	157	1.1807(30)	1.178	1.175
51374.8	$5p_{1/2}7p^3P_0$	3.737	145(6)	106	113			
52265.3	$5p_{3/2}7p^1S_0$	3.128		126	130			
54990.0	$5p_{3/2}7p^1P_1$	3.594	285(10)	171	238	1.0723(21)	1.297	1.153
55139.9	$5p_{3/2}7p^3D_3$	3.627	216(6)	214	163	1.3386(38)	1.292	1.270
55186.9	$5p_{3/2}7p^3P_2$	3.637	193(8)	119	139	1.3073(27)	1.366	1.338
55373.8	$5p_{3/2}7p^3S_1$	3.678	171(5)	154	174	1.8121(43)	1.766	1.777
55500.6	$5p_{3/2}7p^1D_2$	3.708	153(13)	95	108	1.1944(19)	1.132	1.157

^aFrom Moore [2].

^bCalculated by the HFR(A) and HFR(B) models, respectively (see the text).

neutralize the vertical component of the earth's field. These two sets of coils were operated with two high-stability constant-current power supplies. The current has been monitored using a digital multimeter and the current stability was better than 0.1%. The magnetic field calibration was performed by measuring Zeeman quantum beat on the $6s6p^3P_1^o$ level of Yb I, which has a g_J factor value of 1.4928 determined with high precision by Budick and Snir [21] and Baumann and Wandel [22]. The magnetic-field calibration uncertainty was less than 0.1%.

III. MEASUREMENTS AND RESULTS

Due to the Zeeman effect, a degenerate atomic level will split into several sublevels in a magnetic field B . The Zeeman sublevels can be coherently excited by a pulsed laser and, as a result, a temporal modulation of the fluorescence emission will produce Zeeman quantum beats which obviously emerge in time-resolved fluorescence signals. In the experiment, the first-step laser was polarized along the B field to induce a π transition while the second-step laser was polarized perpendicularly to B to get a σ transition. By observing $\Delta M = \pm 2$ quantum beats, the Landé g_J factor can be deduced by the equation $h\omega = 2g_J\mu_B B$, where ω is the frequency of the quantum beats which can be determined by a Fourier transform analysis, μ_B is the Bohr magneton and h is the Planck constant. During the measurements of the Landé factors, in order to conveniently consider the effect of the horizontal component of the earth's field, fluorescence decay curves with quantum beats were recorded in couples respectively under the magnetic fields in opposite direction by switching the current direction in the Helmholtz coils. The average of the two beat frequencies is independent of the horizontal component of the earth's field. For each state, more than six pairs of curves under different field strengths from 5 to 20 G were recorded for the g_J factor measurements, and the mean g_J value was given as the final result in

Table I. The quoted error bars reflect both the statistical scattering of different measurements and a conservative estimate of the possible systematic errors from magnetic field measurements. A typical recording of the fluorescence curve with Zeeman quantum beats is shown in Fig. 3 together with a Fourier transform yielding the beat frequency which is the position of the highest peak (excluding the zero-frequency peak). The peak frequency was determined by fitting a Gaussian shape to the peak. In Fig. 3(b), the sloped background has no effect on the peak frequency result, and the smaller sizable peaks, coming from the tiny waves on the slopes of the quantum beats caused by a weaker fluorescence intensity and from the tail of the quantum-beat curve [Fig. 3(a)] characterized by a bad signal-to-noise ratio, have no physical significance. To obtain better quantum-beat patterns, a polarizer plate was used to filter fluorescence before the grating monochromator.

In order to obtain reliable lifetime values, appropriate experimental conditions were applied to lifetime measurements. A set of Helmholtz coils provided a sufficiently strong magnetic field to wash out quantum beats induced by the geomagnetic field Zeeman splitting for long-lived states. Possible flight-out-of-view effects were specially investigated by changing the slit width and position of the monochromator, and no noticeable effects were observed. To ensure that the measured lifetimes were not affected by radiation trapping, the oven temperature was changed from 1700 to 1400 K to obtain different atomic densities from about 5×10^8 to 1×10^6 cm⁻³. Moreover, the effect of collision deexcitation induced by the interaction between the excited atoms and the residual air molecules in the chamber was examined by decreasing the vacuum by an order of magnitude from around 2×10^{-3} Pa. It was found that the evaluated lifetime values remained constant within the experimental errors. To ensure a linear response of the PMT detector, the recorded fluorescence signals were adjusted to be sufficiently weak and the lifetimes were checked under different signal intensities. Each recording was obtained by averaging

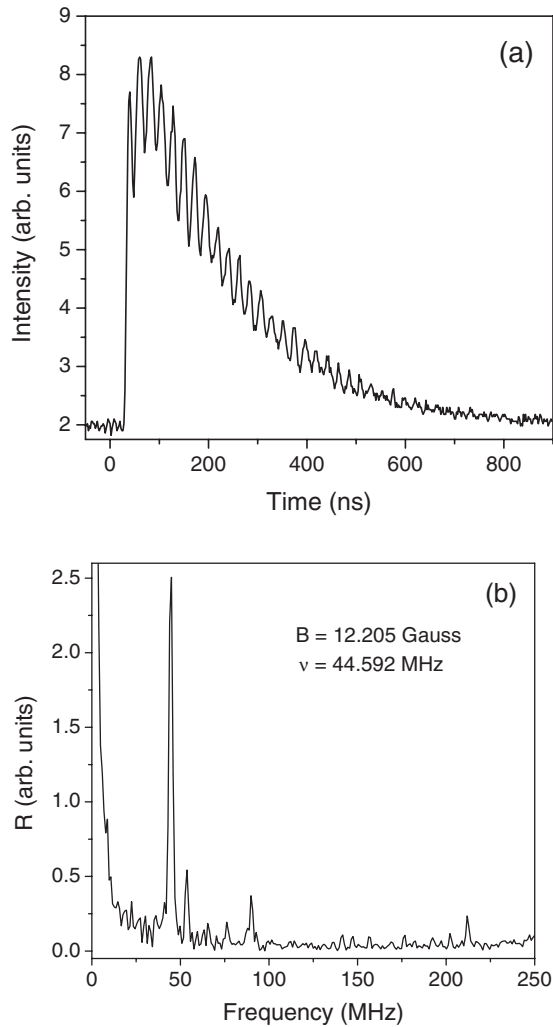


FIG. 3. Zeeman quantum-beat recording (a) and calculated Fourier-transform spectrum (b) for $5p7p^3P_2$.

over 2000 shots to make a smooth curve. A least-squares exponential fitting to the decay part of the recorded fluorescence curves was used to evaluate the lifetimes. A typical fluorescence curve for a lifetime measurement of the $5p7p^3P_2$ state is shown in Fig. 4. Taking into account the constant background in the curve coming from the irradiance of the oven, the fitting function has the form $I = I_0 + A \exp[-(t - t_0)/\tau]$, where I_0 and A are the fitting parameters and τ is the lifetime value, t_0 represents the starting time of fit. There is a more substantial contribution from the stray light of the exciting laser near the peak of the fluorescence curve. An optimum starting point of fit occurs at a well-defined distance from the peak. For the curve in Fig. 4, the optimum value of t_0 can be taken as 200 ns and then we have $I_0 = 2.171(3)$, $A = 12.065(88)$, and $\tau = 190.7(10)$ ns. For each level, about 15–20 fluorescence decay curves were acquired under different experimental conditions and the averaged lifetime value was adopted as the final result. The quoted error bar of the measured lifetimes contains the statistical scattering resulting from the different recordings and the systematic error from fitting calculations. The experimental lifetime results are also listed in Table I.

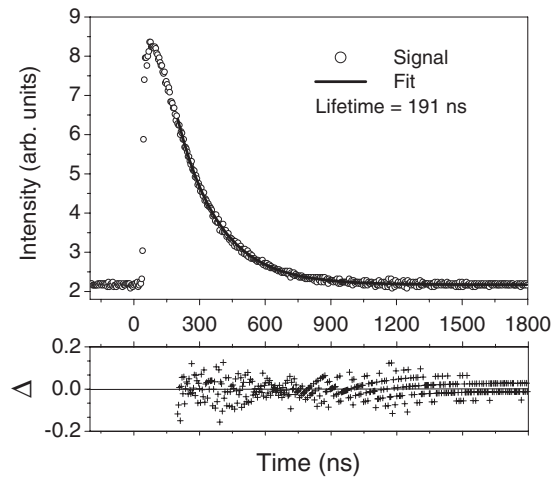


FIG. 4. Typical fluorescence decay curve of $5p7p^3P_2$ with an exponential fitting for lifetime evaluation. The residual plot showing the differences between the data points and the fitted function is shown in the lower figure.

IV. THEORETICAL CALCULATIONS

The experimental radiative lifetimes have been compared with theoretical calculations. For that purpose, we have used a pseudorelativistic Hartree-Fock (HFR) approach [23] in which most of the intravalence correlation is represented within a configuration superposition scheme while core-valence correlation is represented approximately by considering a core-polarization model potential and a correction to the dipole operator as described in detail in [24]. Two sets of calculations were performed. In the first one, HFR(A), outer correlation was retained among the configurations $5s^25p^2$, $5s^25pnp$ ($n=6-10$), $5s^25pnf$ ($n=4-10$), $5s5p^2ns$ ($n=6-10$), $5s5p^2nd$ ($n=5-10$), $5p^3np$ ($n=6-10$), $5p^3nf$ ($n=4-10$), $5p^4$, $5s^25d^2$, $5s^24f^2$, $5s^26s^2$ (even parity) and $5s5p^3$, $5s^25pns$ ($n=6-10$), $5s^25pnd$ ($n=5-10$), $5s5p^2np$ ($n=6-10$), $5s5p^2nf$ ($n=4-10$), $5p^3ns$ ($n=6-10$), $5p^3nd$ ($n=5-10$) (odd parity). The dipole polarizability, α_d , was chosen to be equal to $2.26a_0^3$, as tabulated by Johnson *et al.* [25] for the Pd-like Sn^{4+} ionic core while we used a cutoff radius, r_c , equal to $1.09a_0$ which corresponds to the HFR expectation value of r for the outermost core orbital ($4d$). In calculation HFR(B), the following configuration expansions were considered: $5s^25p^2$, $5s^25pnp$ ($n=6-10$), $5s^25pnf$ ($n=4-10$), $5s^25dns$ ($n=6-10$), $5s^25dnd$ ($n=6-10$), $5s^26sns$ ($n=7-10$), $5s^26snd$ ($n=6-10$), $5s^25d^2$, $5s^24f^2$, $5s^26s^2$ (even parity) and $5s5p^3$, $5s^25pns$ ($n=6-10$), $5s^25pnd$ ($n=5-10$), $5s^25dnf$ ($n=4-10$), $5s^25dnp$ ($n=6-10$), $5s^26snf$ ($n=4-10$), $5s^26snp$ ($n=6-10$) (odd parity). The core polarization effects were estimated using a value of $18.22a_0^3$ for α_d , corresponding to a Cd-like Sn^{2+} ionic core in the tables of Fraga *et al.* [26] and a cutoff radius, r_c , equal to $2.40a_0$ for the outermost core orbital ($5s$).

Using a well-established least-squares fitting procedure [23], the radial parameter values were adjusted to obtain the best agreement between available experimental energy levels and those calculated in both HFR(A) and HFR(B) approaches. More precisely, all of the parameters, i.e., the av-

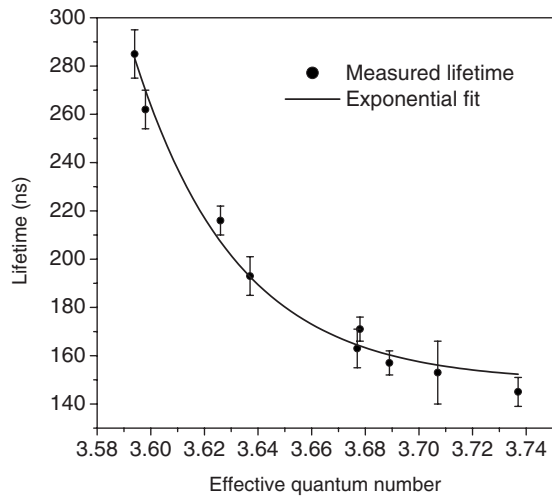


FIG. 5. Measured lifetime values versus effective quantum numbers for $5p7p$ states.

average energies (E_{av}), the Slater integrals (F^k , G^k), the spin-orbit parameters (ζ_{nl}) and the effective interaction parameters (α), were adjusted for the $5p^2$, $5p6p$ even configurations and the $5s5p^3$, $5p6s$ odd configurations in order to better reproduce the observed energy levels. For the $5p7p$, $5p4f$, $5p5f$, $5pns$ ($n=7-10$), and $5pnd$ ($n=5-10$) configurations, only the average energies were fitted. The mean deviations $\Delta E = |E_{\text{expt}} - E_{\text{calc}}|$ were found to be equal to 106 cm^{-1} (even parity) and 205 cm^{-1} (odd parity) for the HFR(A) model and 90 cm^{-1} (even parity) and 192 cm^{-1} (odd parity) for the HFR(B) model.

The theoretical HFR lifetimes and Landé factors calculated for $5p7p$ states by the HFR(A) and HFR(B) models with the adjusted parameters are listed as HFR results in Table I.

V. DISCUSSION

In the present experiment, nine lifetimes and eight Landé g_J factors for the $5p7p$ states in Sn I have been measured using a time-resolved laser spectroscopic technique. For the 1S_0 level, the fluorescence signal was too weak to obtain its radiative lifetime value. Figure 5 shows a plot of the measured lifetime values versus effective quantum numbers n^* of the $5p7p$ states. It can be seen that the lifetimes of these states display an almost exponential decrease with the increase of n^* .

The experimental data available for comparison are extremely sparse. We observe a qualitative agreement with the results deduced from the absolute transition probabilities A_{mn} determined from the arc emission spectra by Wujec and Weniger [27] but their A_{mn} values have errors of about 40%. In addition, it should be mentioned that, among the lifetimes calculated from their A_{mn} values, those for 3D_1 , 3D_2 , and 3P_2 are in good agreement with our experimental results while for some other levels the deviations are larger (discrepancies from 40% up to a factor of 3.15!).

The experimental lifetimes are compared in Table I with the two sets of theoretical data as obtained in the present work, the HFR(B) values being expected to be the more accurate ones due to the fact that a better fit between the calculated eigenvalues of the Hamiltonian and the experimental energy levels is obtained (see Sec. IV). This results from the fact that the interactions between the Sn^{2+} ionic core and the two valence electrons are considered in a more complete way using the HFR(B) core-polarization model than the interactions between the Sn^{4+} and the four valence electrons using the HFR(A) core-polarization model.

It does appear that theory and experiment agree quite well (within 5%) for three levels (at $51\,113.3$, $51\,170.8$, and $55\,373.8 \text{ cm}^{-1}$) and reasonably well (within 20%–30%) for most of the other levels. The largest discrepancies are observed for the two levels at $50\,755.8$ and $55\,500.6 \text{ cm}^{-1}$. A better agreement between theory and experiment for these two levels would probably require for both parities much larger configuration sets but these computations were beyond our computer capabilities. This generally reasonable agreement is gratifying having in mind the difficulties associated with atomic structure calculations in heavy neutral atoms where both relativistic and correlation effects play a role.

Landé g_J factors calculated in intermediate coupling have also been added in Table I. They agree quite well (within a few percent) with the experimental results as obtained in the present work. For the lowest two levels at $50\,755.8$ and $51\,113.3 \text{ cm}^{-1}$, we found that the measured g_J values are rather different by a factor of 2–3 from the values in the pure LS scheme, while for the other levels this kind of deviation is less than 17%. This indicates that the Coulomb interaction is stronger than the spin-orbit interaction except for the $5p_{1/2}7p\ ^3P_1$ and 3D_1 states.

VI. CONCLUSION

We have obtained experimental values for the lifetimes and Landé g_J factors of high-lying even-parity $5p7p$ levels in the Sn atom using a time-resolved laser-induced fluorescence technique and Zeeman quantum-beat spectroscopy. The results obtained agree reasonably well with theoretical results obtained within the framework of the HFR method including some core-polarization effects. The present paper calls for experimental branching fraction determinations for the transitions depopulating the levels measured in the present work in order to obtain relevant sets of transition probabilities.

ACKNOWLEDGMENTS

This work was supported by the National Natural Science Foundation of China (Contract No. 10574056) and by the Program for New Century Excellent Talents in University (China). The author (P.L.) was supported by the National Fund for Fostering Talents of Basic Science (Contract No. J0730311). One of the authors (S.E.Y.) has received a grant from the Belgian DGCD through Grant No. PIC-MAC-1245 and a partial support from the ICTP through Grant No. OEA-AC-71. Financial support from the Belgian National Fund for Scientific Research (FR-FNRS) is acknowledged.

- [1] C. M. Brown, S. G. Tilford, and M. L. Ginter, *J. Opt. Soc. Am.* **67**, 607 (1977).
- [2] C. E. Moore, *Atomic Energy Levels*, Natl. Bur. Stand. (U.S.), Circ. No. 467 (National Bureau of Standards, Washington, DC, 1958), Vol. III.
- [3] W. G. Brill, Ph.D. thesis, Purdue University, 1964.
- [4] J. W. Wilson, Ph.D. thesis, Imperial College of Science and Technology of London, 1964.
- [5] A. Nadeem, A. Ahad, S. A. Bhatti, N. Ahmad, R. Ali, and M. A. Baig, *J. Phys. B* **32**, 5669 (1999).
- [6] A. Nadeem, S. A. Bhatti, N. Ahmad, and M. A. Baig, *J. Phys. B* **34**, 2407 (2001).
- [7] A. Nadeem, S. A. Bhatti, N. Ahmad, and M. A. Baig, *J. Phys. B* **33**, 3729 (2000).
- [8] M. Jin, D. Ding, H. Liu, and S. Pan, *Inst. Phys. Conf. Ser.* **114**, 235 (1990).
- [9] J. Dembczynski and H. Rebel, *Physica B & C* **125**, 341 (1984).
- [10] J. Dembczynski and M. Wilson, *Z. Phys. D: At., Mol. Clusters* **8**, 329 (1988).
- [11] S. Adelman, W. P. Bidelman, and D. Pyper, *Astrophys. J., Suppl.* **40**, 371 (1979).
- [12] I. I. Ivans, J. Simmerer, C. Sneden, J. E. Lawler, J. J. Cowan, R. Gallino, and S. Bisterzo, *Astrophys. J.* **645**, 613 (2006).
- [13] L. Holmgren and S. Svanberg, *Phys. Scr.* **5**, 135 (1972).
- [14] M. Brieger and P. Zimmermann, *Z. Naturforsch. A* **22**, 2001 (1967).
- [15] R. L. de Zafra and A. Marshall, *Phys. Rev.* **170**, 28 (1968).
- [16] G. M. Lawrence, *Astrophys. J.* **148**, 216 (1967).
- [17] N. P. Penkin and I. Yu. Yu. Slavenas, *Opt. Spectrosc.* **15**, 83 (1963).
- [18] E. Back, *Z. Phys.* **43**, 309 (1927).
- [19] J. B. Green and R. A. Loring, *Phys. Rev.* **30**, 574 (1927).
- [20] W. F. Meggers, *J. Res. Natl. Bur. Stand.* **24**, 153 (1940).
- [21] B. Budick and J. Snir, *Phys. Lett. A* **24**, 689 (1967).
- [22] M. Baumann and G. Wandel, *Phys. Lett. A* **28**, 200 (1968).
- [23] R. D. Cowan, *The Theory of Atomic Structure and Spectra* (University of California Press, Berkeley, 1981).
- [24] P. Quinet, P. Palmeri, É. Biémont, M. M. McCurdy, G. Rieger, E. H. Pinnington, M. E. Wickliffe, and J. E. Lawler, *Mon. Weather Rev.* **307**, 934 (1999).
- [25] W. R. Johnson, D. Kolb, and K. N. Huang, *At. Data Nucl. Data Tables* **28**, 333 (1983).
- [26] S. Fraga, J. Karwowski, and K. M. S. Saxena, *Handbook of Atomic Data* (Elsevier, Amsterdam, 1976).
- [27] T. Wujec and S. Weniger, *J. Quant. Spectrosc. Radiat. Transf.* **18**, 509 (1977).